Zero Temperature Dynamics of Ising Systems on Hypercubes

R. Chen[1], J. Machta[2], C.M. Newman[3], and D.L. Stein[4]

[1]*New York University, New York, NY 10012 USA*
[2]*Physics Department, University of Massachusetts, Amherst, MA 010003 USA; Santa Fe Institute, 1399 Hyde Park Road, Santa Fe, NM 87501 USA*
[3]*Courant Institute of Mathematical Sciences, New York University, New York, NY 10012 USA*
[4]*Department of Physics and Courant Institute of Mathematical Sciences, New York University, New York, NY 10012 USA*

Abstract

We study the zero-temperature Glauber dynamics of homogeneous Ising ferromagnets on hypercubes, as their dimension d varies. By letting $d \to \infty$, both numerically and theoretically, we investigate the asymptotic behavior of various features on hypercubes when $t \to \infty$, for example: the final magnetization, the probability for the system to enter ground states, etc. The final states of hypercubes can be divided into 3 categories: the ground states, the frozen states, and the blinker states. We use k-core to describe the geometry of the frozen states and give an exponential lower bound for the number of frozen states in terms of d. Blinker states are final states that contain at least one blinker (permanently flipping spin) and only exist on even dimensions. Blinkers have rich local structures, we give explicit constructions for blinker configurations that contain them and show that the lowest admissible dimension for blinker configurations is $d = 8$. We also study the 'Nature vs. Nurture' problem on hypercubes, asking how much the final state depends on the information contained in the initial configuration, and how much depends on the dynamical evolution. Finally, we give several conjectures and heuristics based on the numerical results.

1 Introduction

For the past 30 years, zero-temperature Glauber dynamics of Ising Systems have been studied on different kinds of graphs both numerically and theoretically, especially on Z^d. For homogeneous Ising ferromagnets on Z^d, If the limit $L \to \infty$ is taken before the limit $t \to \infty$, it has been proven[7, 6] that every spin will flip infinitely many times for $d \leq 2$, and it still remains unproved for $d \geq 3$. If the limit $t \to \infty$ is taken before the limit $t \to \infty$[10, 9, 8], for $d = 1$, there are no frozen states and the system will always enter the ground states; for $d = 2$, besides from entering the ground states, the system can also enter frozen states consisting vertical and horizontal stripes with probability 0.339[1]; for $d \geq 3$, the number of frozen states grows extensively, and there exist permanently flipping spins on sites.

In this paper, we study the zero-temperature dynamics of homogeneous Ising ferromagnets on hypercubes, as their dimension d varies. But L is fixed at 2 on hypercubes, alternatively, we study the asymptotic behaviors of its various features as $d \to \infty$. There are two main properties of hypercubes that benefit our study, the first one is their self-recursiveness — a couple of d-dim hypercubes compose a $(d+1)$-dim hypercube, making configurations easier to describe; the second one is their symmetry — every site are essentially the same. A numerous number of frozen states exist on hypercubes, who eventually trap the dynamics and prevent them from entering the ground states. The geometry of the frozen states is described by 'k-cores', with k satisfying certain dimension requirements. Another interesting feature of the systems studied here is the difference in behavior between odd and even dimensions arising from the presence of zero-energy spin flips in even dimensions and their absence in odd dimensions. In particular, even dimensions can display permanently flipping spins, which we call 'blinkers', which are absent in odd dimensions.

There are two types of randomness in our model, that of the initial configuration and that of the realization of the dynamics. We are interested in the 'Nature vs. Nurture' problem[12, 11] in which one asks how much of the state at time t can be predicted from the information contained in the initial configuration and how much depends on the specific dynamical evolution of the system, all as a function of dimension d.

This paper is organized as follows. In Section 2, the model and methods for studying it are introduced. In Section 3, we present various numerical results on hypercube dynamics, in particular their long-time behavior as a function of dimension. Section 4 focuses on theoretical results regarding the geometries of frozen and blinker states, in particular, we give an exponential lower bound for the number of frozen states, we explicitly construct a blinker configuration at $d = 8$, and show

that the lowest dimension for blinker configurations is also 8. In Section 5, we give several conjectures based on the numerical results and provide some heuristics.

2 Model and Method

We consider a homogenous ferromagnetic Ising system $\sigma_i = \pm 1$ on the sites i of the hypercube $Q_d = \{0,1\}^d$, where the system Hamiltonian for a spin configuration $\sigma \in \{-1,1\}^{Q_d}$ is:

$$\mathcal{H} = -\sum_{\langle i,j \rangle} \sigma_i \sigma_j, \tag{1}$$

with the sum over the nearest neighbors. We denote σ^d as a spin configuration on the d dimensional hypercube; in particular, $\sigma^{d,+}$ and $\sigma^{d,-}$ are the spin configurations of the ground states on the d-dimensional hypercube.

The system is initialized with a random initial configuration constrained to have zero magnetization, each spin is either +1 or -1 with probability $\frac{1}{2}$ and sums up to 0. The hypercube then evolves following zero-temperature Glauber Dynamics: For a single step, we pick a random site i, and compute the energy change ΔE_i that would be caused by flipping the spin at this site (changing S_i to $-S_i$). If $\Delta E_i < 0$, the spin is flipped, if $\Delta E_i > 0$ the spin is not flipped. If $\Delta E_i = 0$, the spin is flipped with probability $\frac{1}{2}$.

We also adopt the algorithm in [12] to accelerate the dynamics, before time t_0, we implement the normal Glauber Dynamic: for each step, we randomly choose a site S_i on the Hypercube, decide whether to flip it or not based on its energy change ΔE_i, and increment time steps by $\frac{1}{2^d}$ after each attempted spin flip. After time t_0, a few of the sites remain active (i.e., $\Delta E_i \leq 0$), in order to speed up the simulation, we implement the Kinetic Monte-Carlo Method: we create an active list $a^d(t)$ for the sites that remain active, for each step we randomly choose a site from the active list and carry out the spin-flip. The difference here is that we now increment time by $\frac{1}{|a^d(t)|}$, where $\left|a^d(t)\right|$ is the length of the active list. After each spin flip, we also need to update the active list by removing the flipped spin and checking whether its neighbor remains active.

The final states can be divided into 3 categories: the ground states, the frozen states, and the blinker states. Frozen states are final states that are stable against single spin flips (i.e., no spins are flippable) but not ground states. Blinker states are final states that contain at least one spin that can flip without energy change forever. Blinker spins exist in works[8] on Euclidean Lattices with $d \geq 3$, and we adopt the name blinker for them. Blinker states only exist on even dimensions, where zero-energy flips ($\Delta E_i = 0$) are possible. A spin σ_i is a 1-blinker if it has an equal number of $+1$ and -1 frozen neighbors. There are many other interesting structures for blinkers, which we will see in Section 4.

The existence of blinkers complicates the notion of a final state and the limit $t \to \infty$. In order to define final states allowing for blinkers we introduce the idea of all dynamically possible futures. Let $G^d(t)$ be the set of all spin configurations that are dynamically accessible starting from the current spin configuration, $\sigma^d(t)$ and running for arbitrarily long times. By construction, $|G^d(t)|$ is not increasing and the limit set G^d_∞ exists, $G^d_\infty = \lim_{t\to\infty} G^d(t)$. For ground states and metastable states, G^d_∞ contains a single spin configuration, but for blinker states, $|G^d_\infty| > 1$. Since the dynamics cannot increase the energy, all configurations in G^d_∞ must have the same energy, and the dynamical transitions between these configurations must be reversible. Thus, the dynamics induce a connected graph, $\mathcal{G}^d = (G^d_\infty, V^d_\infty)$ where the edges V^d_∞ of the graph are the possible energy-conserving single spin-flip transitions between the configurations in G^d_∞. Every configuration in G^d_∞ will be visited infinitely often and with equal probability. Associated with each spin configuration in G^d_∞ is an active list of spins, all of which can be flipped without energy change. The union of all of these active lists is the set of blinkers in the final state, which we refer to as g^d_∞.

In the appendix, we provide an algorithm for testing whether $G^d(t) = G^d_\infty$ and, if so, obtaining G^d_∞. However, for the simulations reported below, we choose a simpler approach. We first run the Kinetic Monte Carlo method for a sufficient time t to ensure that only spins with zero energy change are contained in the active list $a^d(t)$. If $a^d(t)$ is empty, there's nothing for us to do since the hypercube has entered either a ground state or a frozen state. If $a^d(t)$ is not empty, we identify g^d_∞ using a Depth First Search (DFS). Starting with each spin $\sigma^d_i \in a^d(t)$, we examine its neighbors σ^d_j. For each neighbor, we check its energy change ΔE_j. If $\Delta E_j \leq 2$, σ^d_j is a blinker because it can either flip with zero energy cost immediately or after σ^d_i flips. We then recursively apply this process to σ^d_j's neighbors. The DFS stops when all neighbors of the current spin have $\Delta E \geq 2$, as they cannot flip without increasing energy. This approach ensures that all blinkers are efficiently identified through systematic exploration.

Luckily, as we shall see in Section 3, the fraction of the number of blinkers is just of some small order of the whole site. We

investigate the following observables as functions of dimension d, excluding the blinkers:

$$M_\infty(d) = \lim_{t\to\infty} \sum_{i\notin g^d_\infty} \sigma^d_i(t), \tag{2}$$

the magnetization of the final configuration excluding the blinkers;

$$\mathbb{P}_{\sigma(0),\omega}(\{G^d_\infty = \sigma^{d,+} \text{ or } \sigma^{d,-}\}), \tag{3}$$

the probability for a d-dimension hypercube to enter ground states as $t \to \infty$, where the probability is over $\sigma(0)$ the initial configuration and ω the dynamical realization;

$$m^i_\infty(d) = \lim_{t\to\infty} \frac{1}{d} \sum_{\langle i,j\rangle, j\notin g^d_\infty} \sigma^d_j(t), \tag{4}$$

the local magnetization, which is the sum of the neighboring spins of σ^d_i normalized by $\frac{1}{d}$, excluding the blinkers(note that by the symmetry of hypercubes, $m^i_\infty(d)$ is independent of the choice of i, hence we can set i to be the origin $\bar{0}$, and write $m_\infty(d) = m^{\bar{0}}_\infty(d)$ for simplicity);

$$\mathcal{H}_\infty(d) = \lim_{t\to\infty} -\sum_{\langle i,j\rangle} \sigma^d_i(t)\sigma^d_j(t), \tag{5}$$

the energy of the final configuration excluding the blinkers; and $\overline{f(d)}$, the average number of flips per site excluding the blinkers.

To get a deeper study of the frozen states, we introduce the concept of the largest k-core. We first split the final configuration of a d-dim hypercube into two graphs, one consisting of only $+1$ spins, and one consisting of only -1 spins, preserving the edges that connect spins with the same signs and throwing away the edges that connect spins with opposite signs. In each of the graphs, any connected subgraph with all vertices having degrees larger than $k \geq \lfloor \frac{d}{2} \rfloor + 1$ would be frozen. We now ask the problem: What is the size of the largest of these subgraphs? This is actually the problem of finding the largest k-core, where a k-core denotes a connected subgraph with at least k degrees for each vertex in it. We define $\kappa(d) = \max\{k_+, k_-\}$, where $k_\pm$ is the core number for the largest k-core in the ± 1 graph.

We investigate the following two probabilities associated with the blinkers to get a deeper understanding of them. We consider

$$\mathbb{P}_{\sigma(0),\omega}(\{|G^d_\infty| > 1\}), \tag{6}$$

the probability to enter a blinker state, and

$$\mathbb{P}_{\sigma(0),\omega}(\{\sigma^d_i \in g^d_\infty\}), \tag{7}$$

the probability for spin σ^d_i to eventually become a blinker (note that again by symmetry, this probability is independent of the choice of i).

We also study double-copy dynamics, in which we adopt the method in [12], where the authors introduced 'Heritability' to study the Nature vs. Nurture problem. We initialize a pair of systems with the same initial configuration and let each system evolve independently according to the Glauber dynamic. At any fixed time step t, we use parameter

$$q_t(d) = \sum_{i\notin g^d_\infty} \frac{1}{2^d} S^1_i(t) S^2_i(t) \tag{8}$$

to compute the overlap between the two twins, where $S^k_i(t), k = 1, 2$ stands for the state of the ith spin in twin k at time step t. We study the average $\overline{q_t(d)}$ over both the initial configuration and dynamics, and examine

$$\overline{q_\infty(d)} = \lim_{t\to\infty} \overline{q_t(d)}, \tag{9}$$

which is the overlap of the twins at there final states. We are interested in the asymptotic behavior of q_∞ as a function of d when $d \to \infty$, does it go to 1 (Nature wins), or go to 0 (Nurture wins), or somewhere in between?

3 Results

3.1 Single-copy Dynamics

We first present numerical results for $M_\infty(d)$ the magnetization of the final state. Fig. 1 shows the sample distribution of $M_\infty(d)$ normalized by N for different values of d. The first thing to be noticed is the difference between the distributions at even and odd dimensions: distributions at even dimensions are generally broader. But as $d \to \infty$, distribution for both even and odd dimensions concentrate near zero, hinting at a possible central limit behavior as $d \to \infty$.

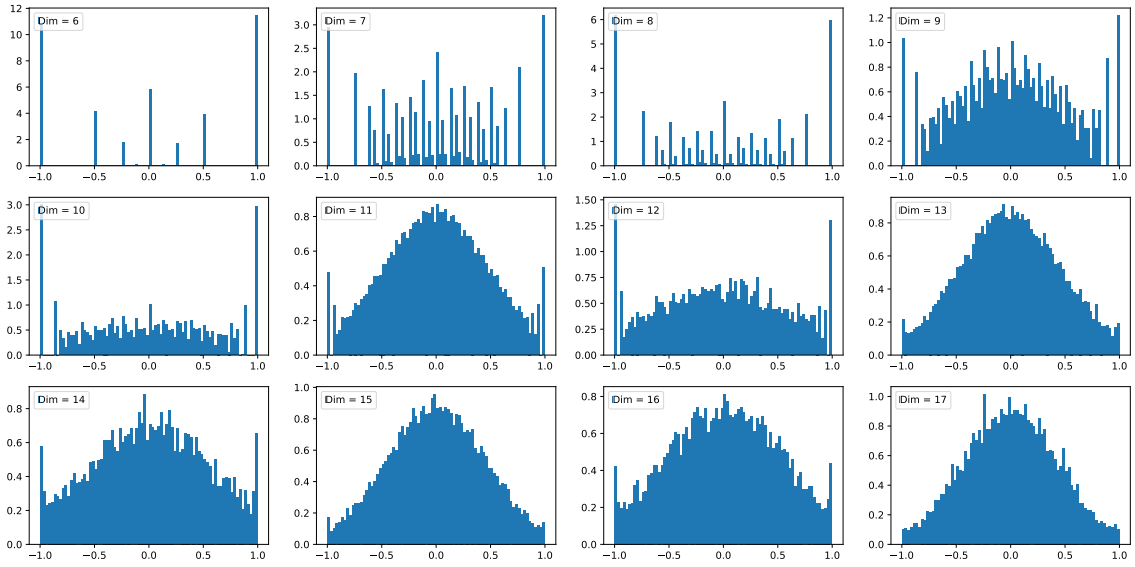

Figure 1: Sample distribution of $M_\infty(d)$ normalized by N at different dimensions

The sum of the two peaks at the ends of the distribution give $\mathbb{P}_{\sigma(0),\omega}(\{G^d_\infty = \sigma^{d,+} \text{ or } \sigma^{d,-}\})$ the probability for the hypercube to enter the ground states as $t \to \infty$. Fig. 2 shows its estimator $\hat{\mathbb{P}}_{\sigma(0),\omega}(\{G^d_\infty = \sigma^{d,+} \text{ or } \sigma^{d,-}\})$ as a function of dimension. $\hat{\mathbb{P}}_{\sigma(0),\omega}(\{G^d_\infty = \sigma^{d,+} \text{ or } \sigma^{d,-}\})$ is larger for even dimensions, but it is decaying to 0 exponentially fast for both even and odd dimensions. Of course, if a CLT on $M_\infty(d)$ is held to be true, this exponential decay would be easy to yield.

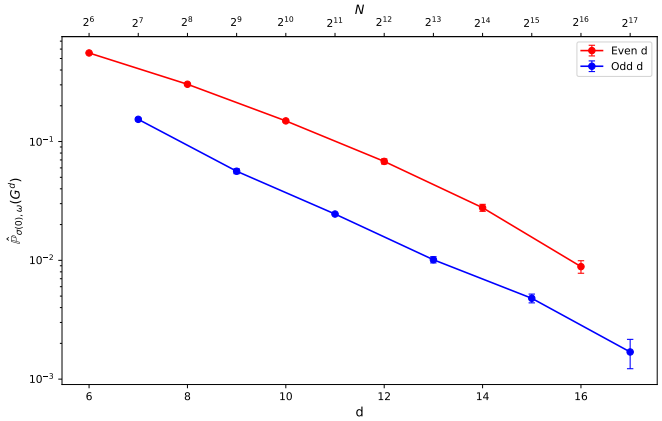

Figure 2: The probability to enter the ground state $\hat{\mathbb{P}}_{\sigma(0),\omega}(\{G^d_\infty = \sigma^{d,+} \text{ or } \sigma^{d,-}\})$ vs. dimensions on a log-linear scale.

Fig. 3a and Fig. 3b show the sample variance of $M_\infty(d)$ scaled by $\sqrt{N}$ and N at different dimensions, both under log scale. One should first notice that as $d \to \infty$, the difference between the sample variance on even and odd dimensions

gradually decreases, suggesting the possible decay of the even-odd disparity. A traditional central limit theorem would have given the scaling factor for the variance of $M_\infty(d)$ to be $\sqrt{N}$, but Fig. 3a shows that the sample variance of $M_\infty(d)$ is actually growing exponentially fast with the dimension when scaled by $\sqrt{N}$. Alternatively, Fig. 3b shows that the sample variance of $M_\infty(d)$ is decaying with the dimension when scaled by N. This actually suggests that the correct scaling factor should be somewhere between $\sqrt{N}$ and N, numerically it suggests $N/\log\log N$, as shown in Fig. 3c.

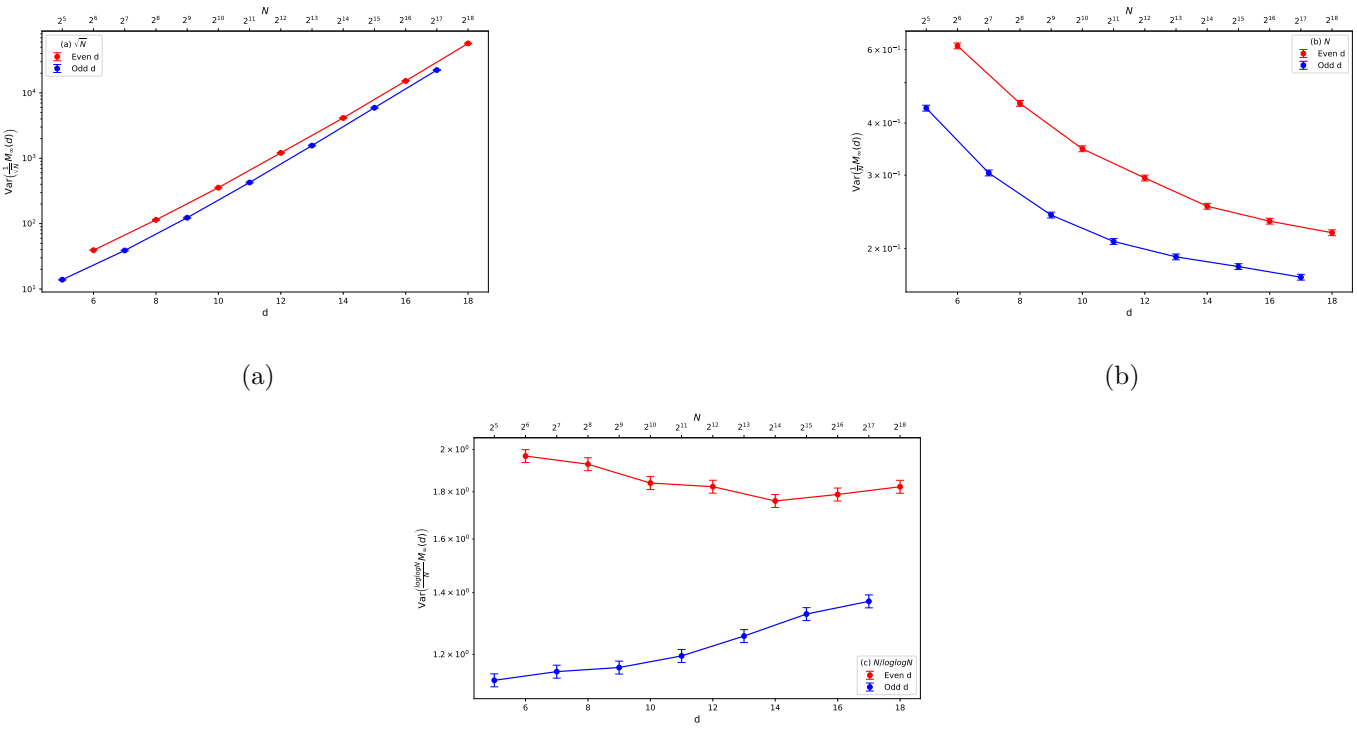

(a) (b)

(c)

Figure 3: Sample variance of $M_\infty(d)$ under three different scales at different dimensions: (a) scaled by $\sqrt{N}$, (b) scaled by N, and (c) scaled by $N/\log\log N$.

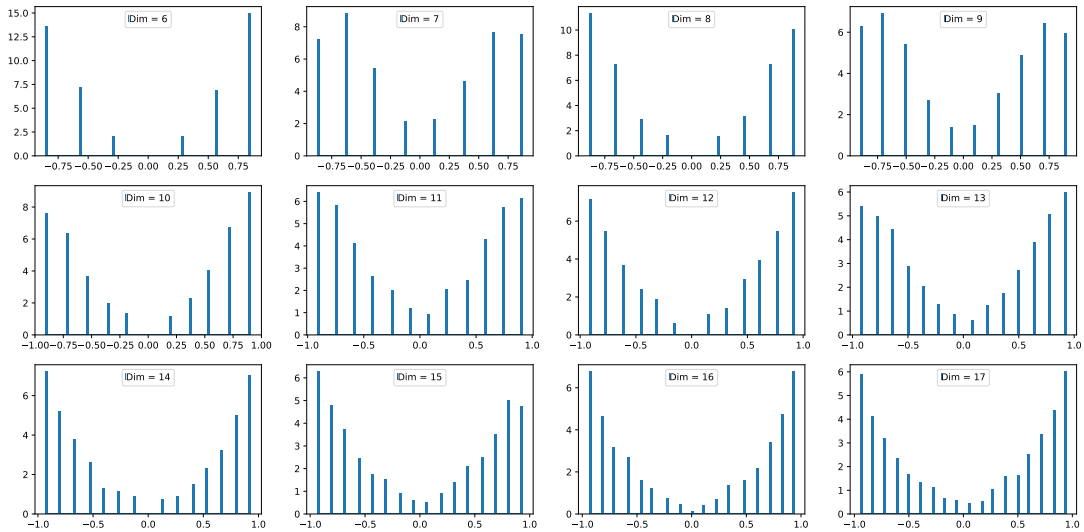

Figure 4: Sample distribution of $m_\infty(d)$ at different dimensions

Alternatively, we can choose to look at $m_\infty(d)$ the local magnetization of the final configuration, which is the sum of all neighbors of the origin. It tells how much a spin can influence its neighbors: Do neighboring spins tend to align with each other or not? Fig. 4 shows the sample distribution of $m_\infty(d)$ at different dimensions d. As d increases, the distribution neither converges to a delta function at 0 (which means zero-correlation between neighboring spins) nor converges to delta functions at $+1$ and -1 (which means neighboring spins align with each other), instead, the distribution is close to a concave-up parabola, with a minimum at 0. Note that on even dimension, the probability mass at 0 exactly corresponds to $\mathbb{P}_{\sigma(0),\omega}(B_i^d)$, the probability for a single site to become a blinker as $t \to \infty$.

Another feature that is closely connected to local magenitization $m_\infty(d)$ is $\mathcal{H}_\infty(d)$, the final energy. Note that the final energy of a spin σ_i equals to $-|m_\infty^i(d)|$, hence one can compute the average final energy based on the distribution of the local magnetization. Fig. 5 shows the sample distribution of mean $\mathcal{H}_\infty(d)$ per site at different values of d. The distribution is generally skewed to the right, and the end of the left tail corresponds to the final energy of the ground states. There is a clear cut-off on the right-hand side, which suggests there is an upper bound on the final energy.

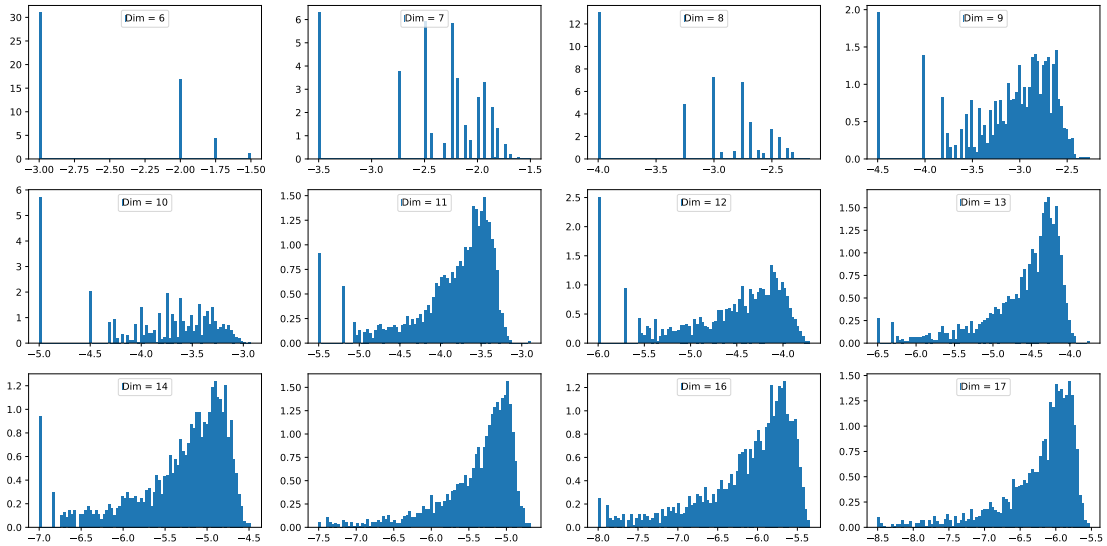

Figure 5: Sample distribution of average $\mathcal{H}_\infty(d)$ per site at different dimensions

Finally, Fig. 6 shows $\overline{f(d)}$ the mean number of flips per site against the dimension, (not counting the blinkers). It's worth noticing that $\overline{f(d)}$ is of small order and grows very slow on both even and odd dimensions, suggesting that most spins on the hypercube require at most a single flip, or none at all, to reach their stable states. $\overline{f(d)}$ on the even dimensions are larger than the odd dimensions, this is because of the existence of 'ties' (i.e, $\Delta E_i = 0$), hence it will generally take more flips for even-dimensional hypercubes to enter a final state.

Many structures on d-dim hypercube can be frozen if fully magnetized (i.e., all spins are of the same sign): k-dim sub-cubes, unions of k-dim sub-cubes (with $k \geq \lfloor \frac{d}{2} \rfloor + 1$), and more generally, k-cores. During dynamics, once such a structure is fully magnetized its size in nondecreasing. These various structures lead to a numerous number of frozen states on hypercubes. And as $d \to \infty$, this number increases rapidly (actually at least on the order of $2^{\sqrt{N}}$). The reason behind $\lim_{d\to\infty} \mathbb{P}_{\sigma(0),\omega}(\{G_\infty^d = \sigma^{d,+} \text{ or } \sigma^{d,-}\}) = 0$ is that the hypercube becomes increasingly likely to get trapped in one of the many frozen states, preventing it from reaching the ground state. For all these frozen states, the largest k-core problem essentially asks: What's the typical largest cluster a frozen state can have?

Fig. 7 shows the sample distribution of $\kappa(d)$ the core number of the largest k-core at different dimensions. Note that $\kappa(d) = d$ is essentially just saying the system has entered the ground. The distribution of $\kappa(d)$ is strictly supported between $\lfloor \frac{d}{2} \rfloor + 1$ to d, this is because no k-cores with a core number smaller than $\lfloor \frac{d}{2} \rfloor + 1$ can survive in the dynamics. We see that as d increases, the distribution is concentrated around $3d/4$, suggesting that a typical largest cluster on a d-dim hypercube will have a core number around $3d/4$. On the other hand, the tails on both sides are going to 0, again the vanish of the left tail corresponds to $\lim_{d\to\infty} \mathbb{P}_{\sigma(0),\omega}(\{G_\infty^d = \sigma^{d,+} \text{ or } \sigma^{d,-}\}) = 0$.

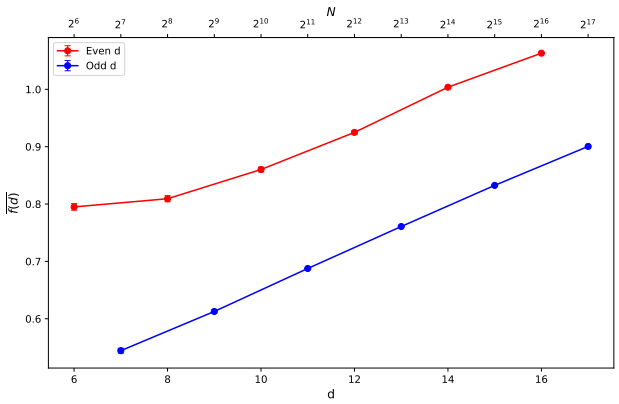

Figure 6: $\overline{f(d)}$ at different dimensions

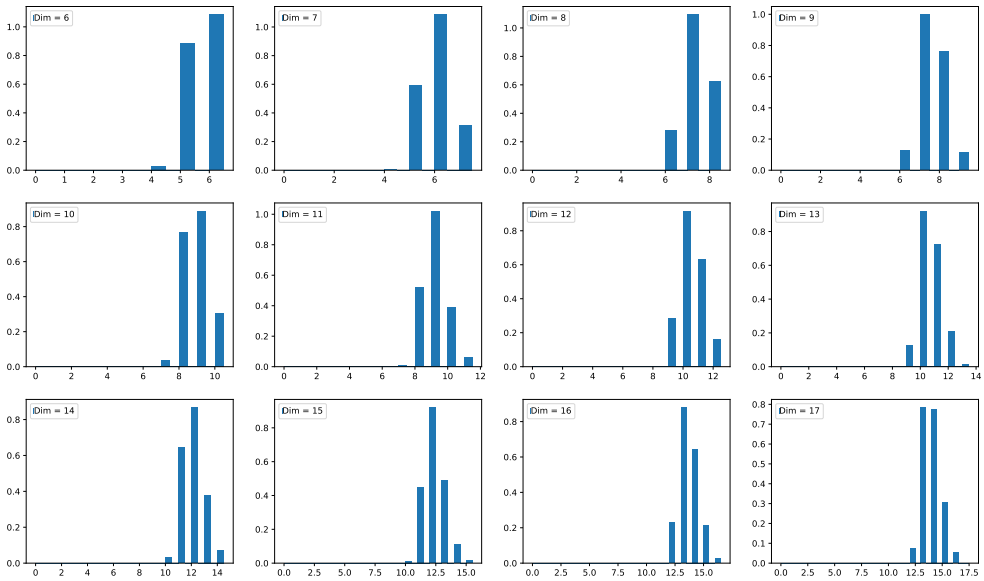

Figure 7: Sample distribution of $\kappa(d)$ at different dimensions

We then inspect the sample mean largest k-core at different dimensions, see Fig. 8 for the linearly fitted plot. Note that the mean of the largest k-core only increments from odd to even dimensions, which is due to the floor function in the dimension requirements $k \geq \lfloor \frac{d}{2} \rfloor + 1$ for stability. Also, the slope parameters (separated on even and odd dimensions) are close to $3/4$, corresponding to the concentration of the largest k-core around $3d/4$.

We finally turn our study to blinkers, the spins that flip permanently as $t \to \infty$, which is another sign of the even-odd difference: only even dimensions allow the existence of blinkers on the final configurations. We first inspect the probability $\mathbb{P}_{\sigma(0),\omega}(\sigma_i^d \in g_\infty^d)$, which is the probability for the spin σ_i to eventually become a blinker. Fig. 9 shows its estimator $\hat{\mathbb{P}}_{\sigma(0),\omega}(\sigma_i^d \in g_\infty^d)$, which is the averaged fraction of the number of blinkers at different dimensions. We see that $\hat{\mathbb{P}}_{\sigma(0),\omega}(\sigma_i^d \in g_\infty^d)$ is growing up slowly with dimensions.

In our experiments, blinkers haven't been observed on any hypercubes with dimensions lower than 8, which in Section 4 we will theoretically show that the lowest dimension requirement is indeed 8. The intuition behind this is that there are certain requirements for the size of the 'surrounding environment' of a blinker. On the other hand, this also means there's repulsion between separated blinkers: if there's already a blinker on the hypercube, there might be not enough space left for another blinker to fit in. Thus alternatively, we consider the conditional probability $\mathbb{P}_{\sigma(0),\omega}(\sigma_i^d \in g_\infty^d || G_\infty^d| > 1)$, that is the

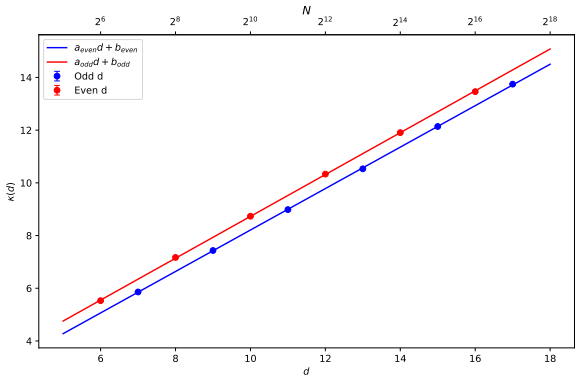

Figure 8: Mean of $\kappa(d)$ at different dimensions, fitting parameters: $a_{even} = 0.794 \pm 0.002, b_{even} = 0.786 \pm 0.020, a_{odd} = 0.786 \pm 0.002, b_{odd} = 0.344 \pm 0.024$

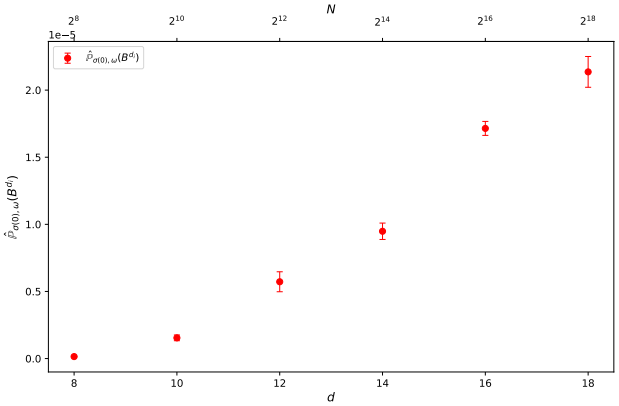

Figure 9: $\hat{\mathbb{P}}_{\sigma(0),\omega}(\sigma_i^d \in g_\infty^d)$ at different dimensions

probability for the spin σ_i to eventually become a blinker conditioned on the event that there is at least one blinker in the hypercube. Fig. 10 shows its estimator $\hat{\mathbb{P}}_{\sigma(0),\omega}(\sigma_i^d \in g_\infty^d || G_\infty^d| > 1)$, which is the averaged fraction of the number of blinkers at different dimensions, throwing away the cases when there're no blinkers, and we use $ad^{-1}2^{-\frac{d}{2}} + b$ to fit it. Now the fraction is decaying, meaning the requirement for the size of the 'surrounding environment' of a blinker is growing with the dimension.

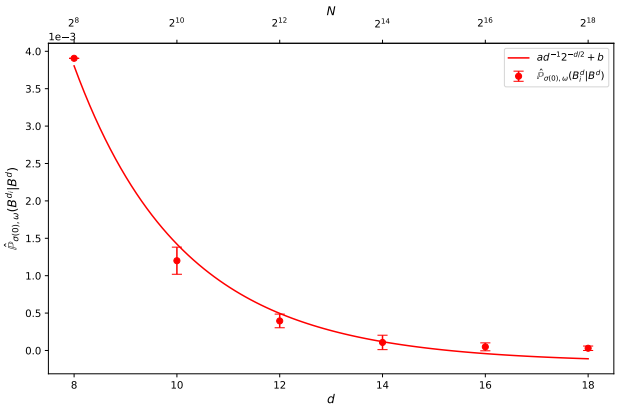

Figure 10: $\hat{\mathbb{P}}_{\sigma(0),\omega}(\sigma_i^d \in g_\infty^d || G_\infty^d| > 1)$ at different dimensions, fitting parameters: $a = 1.97 \pm 0.09$, $b = -1.66 \times 10^{-4} \pm 0.08 \times 10^{-4}$

Finally, we inspect $\mathbb{P}_{\sigma(0),\omega}(|G_\infty^d| > 1)$, the probability for a hypercube to contain at least one blinker. Fig. 11 shows its estimator $\hat{\mathbb{P}}_{\sigma(0),\omega}(|G_\infty^d| > 1)$, which is the frequency of the hypercubes that contains at least one blinker. We see the

frequency is growing exponentially with the dimension, and we believe it will finally reach 1 as $d \to$. This means that large even dimensional hypercubes, with probability one, will contain at least one blinker. But thankfully by the decay of $\mathbb{P}_{\sigma(0),\omega}(\sigma_i^d \in g_\infty^d || G_\infty^d | > 1)$, we know the blinkers will just be a small fraction.

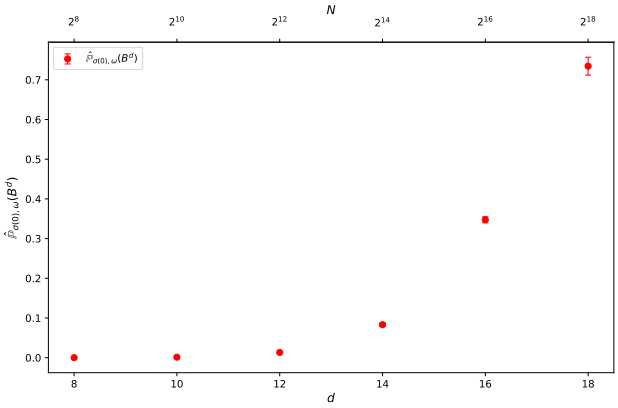

Figure 11: $\hat{\mathbb{P}}_{\sigma(0),\omega}(|G_\infty^d| > 1)$ at different dimensions

3.2 Double-copy Dynamics

We then turn our study to $q_\infty(d)$, the final overlap between a couple of twins starting with the same initial configuration. Fig. 12 shows the sample distribution of $q_\infty(d)$ at different dimensions. The first thing to be noticed is that similar to the final magnetization, the distribution of $\overline{q_\infty(d)}$ is generally broader on even dimensions. The distribution of $q_\infty(d)$ is generally skewing to the right, and it neither concentrates around 1, meaning the information contained in the initial configuration will be completely preserved by the dynamics (which is indeed the case on diluted Curie-Weiss Model[2]), nor concentrates around 0, meaning the initial information will be worn out by the dynamics, $q_\infty(d)$ is gradually concentrating around 0.5 as d grows.

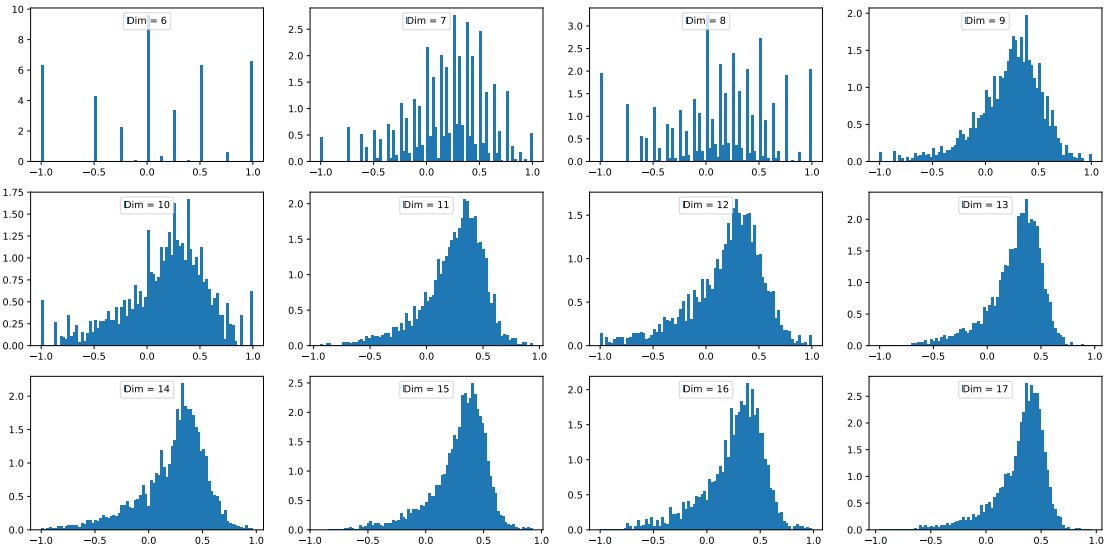

Figure 12: Sample distribution of $q_\infty(d)$ at different dimensions

To examine the limit of $q_\infty(d)$ as $d \to \infty$, we examine its sample mean $\overline{q_\infty(d)}$. Again $\overline{q_\infty(d)}$ is alternatively increasing between even and odd dimensions. Fig. 13 and Fig. 14 showed two fits for $\overline{q_\infty(d)}$ using the simple power law: $c - a * d^b$. c

is the asymptotic parameter which takes in value between 0 and 1. The even-odd difference also suggests using two different power laws with the same asymptotic parameter c to fit our data. There are also two choices for the power parameter b, we can set b to be shared across even and odd d(Fig. 13), or we can set b_{odd} and b_{even} separately(Fig. 14), we hereby examine both.

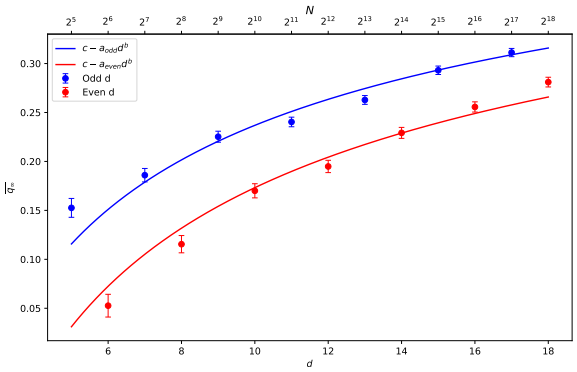

Figure 13: Sample mean of $\overline{q_\infty(d)}$ at different dimensions, fitted with same power parameters on even and odd dimensions: $a_{even} = 1.13 \pm 0.09, a_{odd} = 0.95 \pm 0.04, b = -0.44 \pm 0.18, c = 0.58 \pm 0.14$

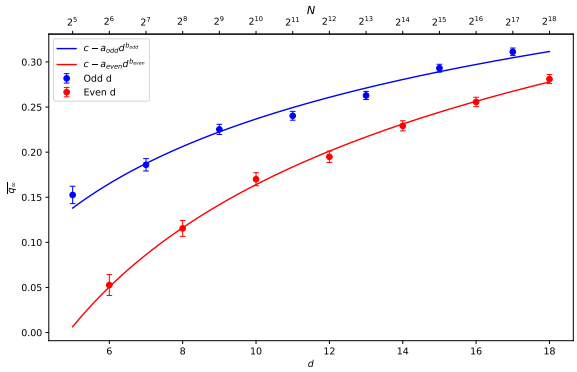

Figure 14: Sample mean of $\overline{q_\infty(d)}$ at different dimensions, fitted different power parameters on even and odd dimensions: $a_{even} = 1.48 \pm 0.05, a_{odd} = 1.12 \pm 0.06, b_{even} = -0.25 \pm 0.02, b_{odd} = -0.17 \pm 0.01, c = 1.00^{+0.00}_{-0.06}$

It's interesting that choosing to share power parameter b or not yields two different asymptotic values for $\overline{q_\infty(d)}$. When setting b to be shared, the fitting suggests $\overline{q_\infty(d)} \to 0.58 \pm 0.14$, corresponding to the concentration of $q_\infty(d)$ around 0.5 we've seen previously in Fig. 12. When setting b separately, the fitting suggests $\overline{q_\infty(d)} \to 1$, but given the large entropy of the metastable states, it's counterintuitive for $q_\infty(d)$ to go to 1

4 Theoretical Results and Constructions

4.1 Frozen States

We begin this section with a definition of a renormalization operation that exploits the recursive structure of the hypercubes and reduces the dimensionality of the resulting structure, which turns out to be very useful when proving facts on hypercubes.

Definition 1. *A **k-renormalization** on the hypercube Q_d is defined as the mapping of Q_d onto a lower-dimensional hypercube $\tilde{Q}_{d-k}$, where:*

1. *Each vertex i of $\tilde{Q}_{d-k}$ is associated to a k-dimensional sub-cube $Q_{k,i}$.*
2. *Each edge between two vertices i and j in $\tilde{Q}_{d-k}$ is associated to k edges connecting the vertices of $Q_{k,i}$ and $Q_{k,j}$. Specifically, these edges connect every site in $Q_{k,i}$ to the corresponding site in $Q_{k,j}$.*

Remark: Such a renormalization is only unique up to permutation, one can fix $d-k$ arbitrary coordinates to be the vertices j, while free the other k coordinates to be the contents inside each sub-cube $Q_{k,j}$. Hence one can have $\binom{n}{k}$ number of such renormalization. We first present a construction that allows one to combine two arbitrary d-dim stable configurations into a $(d+2)$-dim stable configuration.

Theorem 2. *Given any two final states d-dim ($d \geq 3$) configurations $\sigma^{d,a}, \sigma^{d,b} \in \{-1,1\}^{Q_d}$, then through a 2-renormaliztion, the following two $(d+2)$-dim configurations are also final states:*

$$\sigma^{d+2,1}_{(i,i_{d+1},i_{d+2})} = \begin{cases} \sigma_i^{d,a} & \text{if } (i_{d+1},i_{d+2}) = (0,0), \\ \sigma_i^{d,+} & \text{if } (i_{d+1},i_{d+2}) = (0,1), \\ \sigma_i^{d,-} & \text{if } (i_{d+1},i_{d+2}) = (1,0), \\ \sigma_i^{d,b} & \text{if } (i_{d+1},i_{d+2}) = (1,1), \end{cases} \quad \text{(a.1)}$$

$$\sigma^{d+2,2}_{(i,i_{d+1},i_{d+2})} = \begin{cases} \sigma_i^{d,a} & \text{if } (i_{d+1},i_{d+2}) = (0,0), \\ \sigma_i^{d,b} & \text{if } (i_{d+1},i_{d+2}) = (0,1), \\ -\sigma_i^{d,a} & \text{if } (i_{d+1},i_{d+2}) = (1,0), \\ -\sigma_i^{d,b} & \text{if } (i_{d+1},i_{d+2}) = (1,1), \end{cases} \quad \text{(a.2)}$$

where $i \in Q_d$ *and* $(i_{d+1}, i_{d+2}) \in \{0,1\}^2$.

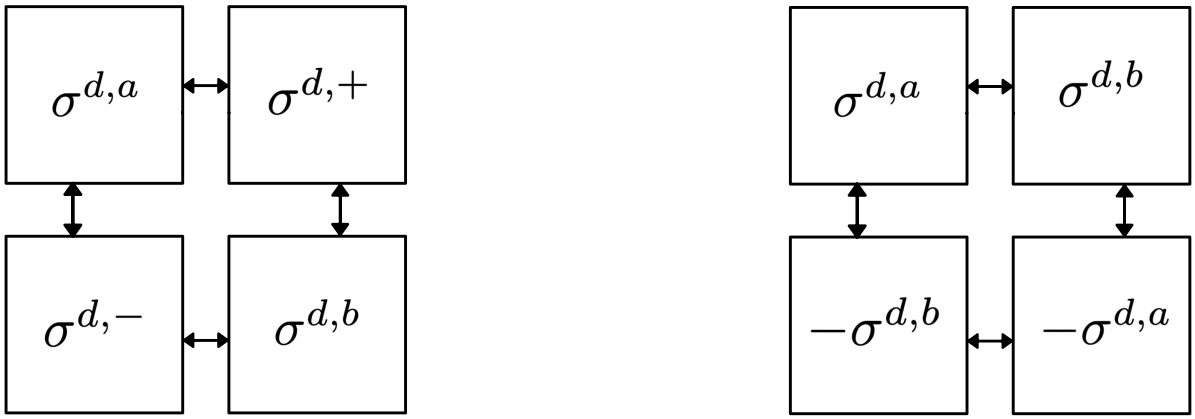

(a) (b)

Figure 15: Graphs for constructions in Theorem 2, (a): $\sigma^{d+2,1}$, (b): $\sigma^{d+2,2}$, each square represents a d-dim hypercube, a double-headed arrow between two hypercubes means connections between all spins with same coordinates.

Proof. We consider the energy change ΔE^{d+2} for each spin in $\sigma^{d+2,1}$. For $i \in Q_k$, if $i' = (i,0,0)$, we have $\Delta E^{d+2}_{i'} = \Delta E^d_i > 0$, since $\sigma^{d+2,1}_{i'}$ is only additionally connected to a plus spin and a minus spin compared to $\sigma^{d,a}_i$. Similarly, $\Delta E^{d+2}_{i'} > 0$ if $i' = (i,1,1)$. Now if $i' = (i,1,0)$ or $(i,0,1)$, $\Delta E^{d+2}_{i'} \geq \Delta E^d_i - 2 > 0$. Hence $\sigma^{d+2,1}$ is a final state. $\sigma^{d+2,2}$ can be proved to be a final state similarly. □

Suppose the number of d-dim frozen states is n. By Theorem 2, both $\sigma^{d,a}$ and $\sigma^{d,b}$ have n choices, therefore the number of $(d+2)$-dim metastable states should be at least n^2. Hence one should expect the number to grow as $2^{2^{\frac{d}{2}}} = 2^{\sqrt{N}}$. In general, frozen states enjoy abundant structures on hypercubes. The simplest way to construct a frozen state on a d-dim hypercube Q_d is as follows:

Example 3. *For* $k \geq \lfloor \frac{d}{2} \rfloor + 1$*, consider the* k*-renormalization of* Q_d *into* $\tilde{Q}_{d-k}$*, so that each vertex* j *of* $\tilde{Q}_{d-k}$ *is a* k*-dim sub-cube* $Q_{k,j}$*. Fix* $j_0 \in \{0,1\}^{\tilde{Q}_{d-k}}$*, set all spins in* Q_{k,j_0} *to be plus, and all spins in* Q^c_{k,j_0} *to be minus. Then this is a frozen state.*

Proof. Each spin in Q_{k,j_0} has k plus neighbors and $d-k$ minus neighbors, hence is stable. There are d sub-cubes $Q_{k,j}$ that are connected to Q_{k,j_0}, where $d_h(j,j_0) = 1$, d_h is the Hamming distance. For each such j, all spins in $Q_{k,j}$ have 1 plus neighbors and $d-1$ minus neighbors, hence is also stable. Since the rest of the spins only have minus neighbors, this is a metastable state. □

We now prove the lower bound for the number of frozen states, in the same manner of Example 3, through which we exploit the dimension requirement for stability to the largest extent.

Theorem 4. *Let* $\mathcal{F}^d = \{\sigma^d \text{ frozen}\}$*, we have* $|\mathcal{F}^d| = \Omega(2^{\sqrt{N}})$

Proof. For the sake of simplicity, assume d even. We first $\frac{d}{2}+1$-renormalize Q_d into $\tilde{Q}_{\frac{d}{2}-1}$, so that each vertex j of $\tilde{Q}_{\frac{d}{2}-1}$ is a $(\frac{d}{2}+1)$-dim sub-cube $Q_{\frac{d}{2}+1,j}$. For each j, set the spins in $Q_{\frac{d}{2}+1,j}$ to be either all plus or all minus. Then each spin in $Q_{\frac{d}{2}+1,j}$ will have at least $\frac{d}{2}+1$ neighbors that agree with it, therefore must be frozen. In total there are $2^{\frac{d}{2}-1}$ such sub-cubes, hence there are at least $2^{2^{\frac{d}{2}-1}}$ of frozen configurations. □

But such construction in Theorem 4 is not the only possible frozen structure in a frozen configuration. Any structure that is a k-core is frozen, hence as long as k satisfies the dimension requirement $k \geq \lfloor \frac{d}{2} \rfloor + 1$, in principle any configuration in which the set of plus spins (and similarly minus spins) is a union (not necessarily disjoint) of sub-cubes Q_k would be a frozen configuration. One then may ask: does there exist a frozen state that violates this rule? The answer is yes, and such a violation starts to exist in surprisingly low dimensions.

Example 5. *On a* 5*-dim hypercube* Q_5*, set all the spins on the sites in Fig. 16 to be plus, and set all the remaining spins to be minus. Then this is a frozen configuration, and the set of plus sites contains no 3-cube as a subset and similarly, the set of minus sites contains no 3-cube as a subset.*

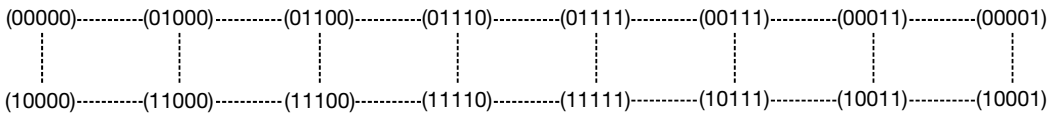

Figure 16: Coordinates of the plus spins in Q_5 that contains no 3-cubes

The graph of the plus spins can be viewed as a ring of 8 two-site sets. In fact, its complement, the graph of the minus spins shares exactly the same structure of it (See Fig. 17 for a visualization). Both of them are frozen since each spin has 3 neighbors that agree with. Hence we've constructed a frozen configuration in which the set of plus(minus) spins is only a union of $Q_{\lfloor \frac{d}{2} \rfloor}$'s.We can also do a similar 2-renormalization on Q_6, but instead, we will have $Q_{2,j}$ on each vertex j of $\tilde{Q}_4$, this is also a frozen state with no 4-cubes contained. This construction starts to collapse on Q_7, which contains 4-cubes. What

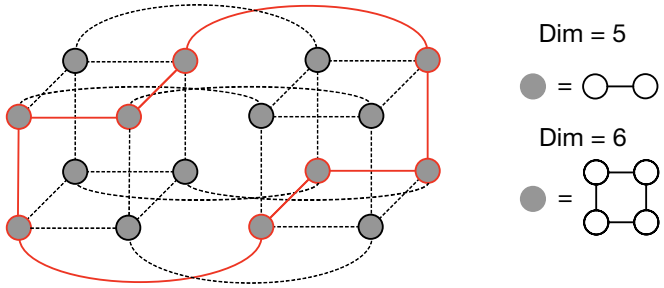

Figure 17: Visualization for Q_5 in Fig. 16 1-renormalized into $\tilde{Q}_4$, with a 1-dim sub-cube $Q_{1,j}$ on each vertex j. A red-filled circle stands for a 1-dim plus sub-cube (i.e.: two connected points), and a black-filled circle stands for a 1-dim minus sub-cube. The red edges are the edges between plus spins, and the dashed edges are the other edges. The red loop is the structure described in Fig. 16. Similarly, one can form a black loop only using the minus spins.

if we want to construct a metastable configuration in which the set of plus(minus) spins is only a union of $Q_{\lfloor \frac{d}{2} \rfloor - a}$'s? Since the dimension in each sub-cube is lower, we should require a higher dimension for the structure connecting them. We first consider the $Q_{\lfloor \frac{d}{2} \rfloor - 1}$ case, in which we choose a two-dim torus as an analog of the ring structure in Example 5:

Example 6. *On a 7-dim hypercube Q_7, set all the spins on the sites in Fig. 18 to be plus, and set all the remaining spins to be minus. Then this is a metastable configuration, and the set of plus sites contains no 3-cube as a subset.*
Remark: Different from Example 5, the set of minus spins here contains 4-cube.

Figure 18: Coordinates of the plus spins in Q_7 that contains no 4-cubes

Similarly as before, we can do a renormalization on Q_8, and assign each site in Fig. 18 to be a 1-d sub-cube $Q_{1,j}$, which attains a metastable state with no 4-cubes contained. Thus in principle, in order to construct a metastable state in which

the set of plus(minus) spins is only a union of $Q_{\lfloor \frac{d}{2} \rfloor - a}$'s, we can choose the structure connecting them to be an $(a+1)$-dim torus embedded in Q_d. Finally, to ensure a successful embedding, let l_i be the length of the torus in the i-th dimension, we require [4]:

$$\sum_{i}^{a+1} \lfloor \log_2(l_i) \rfloor \leq d \tag{10}$$

4.2 Blinker States

We begin this section with a construction of a blinker configuration consists a 1-blinker using unions of sub-cubes. To make things easier, we suppose we are at the lowest dimension we observed blinker configurations in our experiment: $d = 8$, but one should note that similar construction can be applied to any even $d \geq 8$. Let $\vec{0}$ the origin be the site for the blinker. We know that it has 4 plus neighbors and 4 minus neighbors. We assume spins at the sites (1000|0000), (0100|0000), (0010|0000), (0001|0000), to be plus, and spins at the sites (0000|1000), (0000|0100), (0000|0010), (0000|0001) to be minus.

The construction goes as follows, at $t = 0$, for each plus neighbor, choose a 5-dim sub-cube including the plus neighbor and make it all plus; for each minus neighbor, choose a 5-dim sub-cube including the minus neighbor and make it all minus. At the same time, we should carefully pick these sub-cubes such that there's no overlap between the plus ones and the minus ones. Finally, set the spin values in the complement of the union of these eight 5-dim sub-cubes to be arbitrary. Let the above initial configuration evolve through the dynamics, the union of plus sub-cubes and minus sub-cubes are frozen at $t = 0$, then as $t \to \infty$, we'll obtain a blinker configuration, and the spin on $\vec{0}$ will become a 1-blinker.

We use the notation * for a coordinate that can be either 0 or 1, hence a 5-dim sub-cube containing (0100|0000) can be written as (*1**|**00). Here's a possible selection of the four plus 5-dim sub-cubes and four minus 5-dim sub-cubes that have no overlap:

four plus 5-dim sub-cubes: (1***|00**), (*1**|**00), (**1*|00**), (***1|**00).

four minus 5-dim sub-cubes: (*0*0|1***), (*0*0|*1**), (0*0*|**1*), (0*0*|***1).

In particular, if we simply set the complement of the union of the four plus 5-dim sub-cubes above to be all minus, we'll immediately gain a blinker configuration at $t = 0$, again with a 1-blinker on $\vec{0}$. This is because the complement, except for the origin, is also a union of minus 5-dim sub-cubes, and thus is also frozen. A more detailed proof is given in the Appendix.

The existence of blinkers is heavily dependent on their local environment, especially their nearest neighbor and next nearest neighbor, and thus the dimension. One can then ask: What's the lowest dimension for a single-site blinker to exist?

Theorem 7. *There exists no blinker configurations on a d-dim hypercube Q_d, for $d < 8$.*

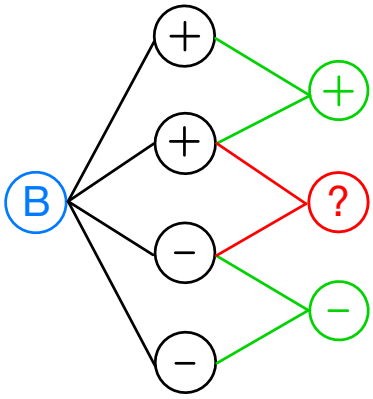

Figure 19: Counting argument for the existence of a single-site blinker. The blue circle is the single-site blinker. The black circles are the nearest neighbors (NN). The green circles are the like next nearest neighbors (like-NNN). The red circle is the unlike next nearest neighbors (unlike-NNN)

Proof. Consider we are at $dim = d$. Each site has d nearest neighbors (NN), and $d(d-1)/2$ next nearest neighbors (NNN) (See Fig. 19). A single-site blinker must have $\frac{d}{2}$ NN to be $+1$ and $\frac{d}{2}$ NN to be -1. To make sure each of its NN's is stable, we must require $\frac{d}{2}+1$ number of NNN to agree with it. We may further assume the spin of the NNN of two NN's having the same spin also agrees with them, we name it to be the like-NNN, and otherwise unlike-NNN. Each NN has $\frac{d}{2}-1$ like-NNN's,

hence it requires two more unlike-NNN's to be stable. Therefore in total, we require $2d$ distinct number of unlike-NNN's. The total number of unlike-NNN is $\frac{d^2}{4}$, hence we have the following inequality: $2d \geq \frac{d^2}{4}$, which gives $d \geq 8$. □

We can use a similar counting argument (See Appendix) to prove that the dimension requirement for a two-site blinker is $d^2 - 8d + 4 \geq 0$, which gives the inequality $d \geq 7.46$. It's surprising that the counting argument for the double blinker is weaker than for the single blinker, but the environment required for a two-site blinker to exist should be stricter than a single blinker. Provided that a double-blinker has never been observed at $d = 8$ in our experiment, it might be the case that the counting argument here only serves as a lower bound, but the true dimension for a two-site blinker to exist should be 10.

In our experiments, we've observed blinkers with different kinds of structures, to appreciate the geometry of different blinker structures, we first present a couple of examples illustrating the dynamics. Fig. 20 shows the local configuration of a 2-blinker and its dynamics. Fig. 21 shows the local configuration of a tree blinker and its dynamics. In Example 8, we present an explicit construction of a blinker configuration containing a 2-blinker on a 10-dim hypercube using a 2-renormalization. Note that one can repeat this construction to obtain an n-blinker, and similar approach can be used to construct a blinker configuration contains a tree blinker.

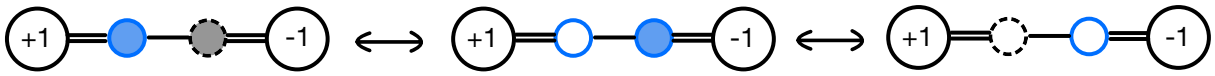

Figure 20: Illustration for the local configuration of a double-site blinker and its dynamics. Filled circles are plus spins and empty circles are minus spins. Blue circles are spins that are currently free to flip. Dashed circles are spins that are currently frozen, but can potentially become free to flip in the future. Any spin connected to a circle filled with $+a$ by a double line must have exactly a more plus neighbors than minus neighbors, and $-a$ means a more minus neighbors than plus neighbors. Each state commutes with the states next to them.

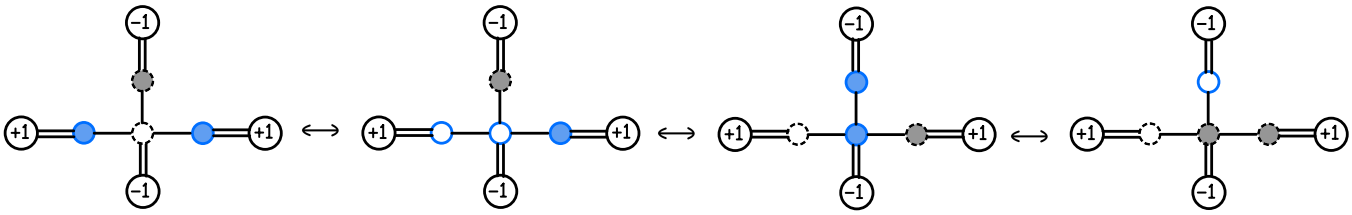

Figure 21: Illustration for the local configuration of a tree blinker and its dynamics. Each state commutes with the states next to them.

Example 8. *The final configuration $\sigma^{10,2b}$ in (4) gives a blinker configuration containing a 2-blinker on a 10-dim hypercube Q_{10}, where $\sigma^{8,d}$ is a blinker configuration containing a 1-blinker on a 8-dim hypercube.*

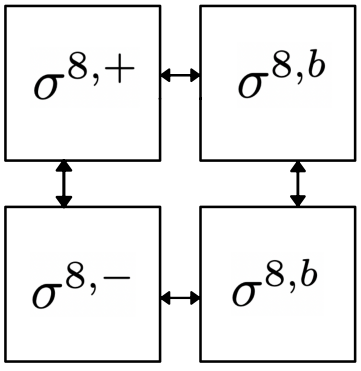

$$\sigma^{10,2b}_{(i,i_9,i_{10})} = \begin{cases} \sigma_i^{8,+} & \text{if } (i_9, i_{10}) = (0,0), \\ \sigma_i^{8,b} & \text{if } (i_9, i_{10}) = (0,1), \\ \sigma_i^{8,-} & \text{if } (i_9, i_{10}) = (1,0), \\ \sigma_i^{8,b} & \text{if } (i_9, i_{10}) = (1,1), \end{cases} \tag{b}$$

where $i \in Q_8$, and $(i_9, i) \in \{0,1\}^2$

Figure 22: Graphs for constructions in Example 8, each square represents an 8-dim hypercube, a double-headed arrow between two hypercubes means connections between all spins with the same coordinates. In particular, the 1-blinker in the upper right sub-cube is connected to the 1-blinker in the bottom right sub-cube. The plus sub-cube and the minus sub-cube are obviously stable. Except for the 1-blinker, each of the spins in the upper right sub-cube gains an extra spin aligning with it by attaching to the bottom right sub-cube, hence will remain frozen when attaching to the plus sub-cube. Similarly, each of the spins in the bottom right sub-cube will remain frozen. The 1-blinker in the upper right sub-cube gains an extra plus spin, and the 1-blinker in the bottom right sub-cube gains an extra minus spin, together forming a 2-blinker.

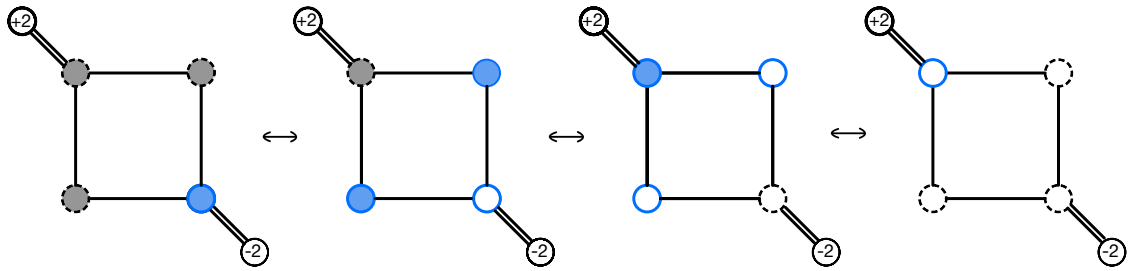

Figure 23: Illustration for the local configuration of a loop blinker and its dynamics. Each state commutes with the states next to them.

Given Theorem 7, we can actually construct a loop blinker at $d = 10$. Fig. 23 shows the structure for a simple loop blinker, the site on the top left corner has 2 more plus neighbor spins than minus neighbor spins, correspondingly, the site on the bottom right has 2 more minus neighbor spins. The sites on the top right and bottom left have an equal number of plus and minus neighbor spins. These four spins together form a loop blinker by connecting as in the way in the figure. An example dynamic (see Fig. 23)for the loop blinker is as follows: Assume all the four spins are $+1$ at the beginning, then the spin on the bottom left can do a zero-energy flip, which changes into -1. But now the spins on the top right and bottom left can both do a zero-energy flip. If both of them change into -1, the top left spin can finally do a zero-energy flip. Now the four spins have changed from all $+1$ to all -1.

We now present a construction for a blinker configuration containing such a loop blinker on Q_{10}. We first pick a metastable configuration $\sigma^{8,a}$ with a specific site i having 5 plus neighbor spins and 3 minus neighbor spins (to construct such a configuration, consider a 5-renormalization of an 8-dim hypercube, with a 5-dim sub-cube on each vertex j of $\tilde{Q}_3$. Fix $j_0 \in \tilde{Q}_3$, and set sub-cube $\tilde{Q_{3,j}}$ to be all plus, and set the complement to be all minus. This is the desired frozen configuration). Then by Theorem 7, we are able to pick a blinker configuration $\sigma^{8,b}$ with a single blinker at site j on Q_8. By rotation invariance of the hypercube, without loss of generality, we can assume $i = j$. Now by construction (2.2) in Theorem 2, we can combine these two configurations into a configuration σ^{10} on Q_{10}. We see that now the single blinkers, the spin on site i, and their flipped spins form a loop blinker.

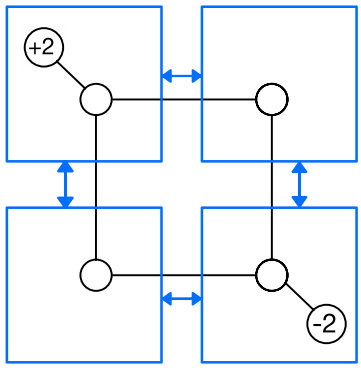

Figure 24: Construction for a blinker configuration that contains a loop blinker by four Q_8's. The upper right Q_8 is a blinker configuration $\sigma^{8,b}$ that contains a 1-blinker on site i. The bottom left Q_8 is the spin-flipped version of $\sigma^{8,b}$. The upper left Q_8 is a frozen configuration $\sigma^{8,a}$, with site i having 5 plus neighbors and 3 minus neighbors. The bottom right is the spin-flipped version of $\sigma^{8,a}$.

5 Discussion

In this section, we present several conjectures inspired by our numerical results and support them with plausible arguments.

Conjecture 1. *The probability for a d-dim hypercube to enter ground state goes to zero as $d \to \infty$, i.e.:*

$$\lim_{d\to\infty} \mathbb{P}_{\sigma(0),\omega}(\{G^d_\infty = \sigma^{d,+} \text{ or } \sigma^{d,-}\}) = 0. \tag{11}$$

Numerical results (Fig. 2) strongly support this, in fact, it suggests $\mathbb{P}_{\sigma(0),\omega}(\{G^d_\infty = \sigma^{d,+} \text{ or } \sigma^{d,-}\})$ should decay to 0 exponentially fast. Theorem 4 shows that the number of frozen states grows exponentially fast with a power factor of $2^{\frac{d}{2}}$. On large d, the large number of frozen states will trap the dynamics, and prevent the hypercube from entering the ground states. Hence one should expect the probability for a d-dim hypercube to enter ground states will go to zero as $d \to \infty$.

Now take d large enough, suppose the probability for a d-dim hypercube to enter ground states is p. We know p is strictly between 0 and 1, since there's positive probability for the hypercube to either start with a frozen state or a ground state. If we run dynamics on two uncoupled d-dim hypercubes, the probability for the whole system to enter ground states is apparently p^2. Now consider a $(d+1)$-dim hypercube being composed by two d-dim sub-cubes, coupled in the sense that each corresponding sites are connected. Alternatively, if we run dynamics on the $(d+1)$-dim hypercube, we should expect them not to variate too much from the uncoupled dynamics, because the density of perturbable spins — one for which a single additional spin connected to it could change whether it flips or the direction it flips, is sufficiently small for large d. Consequently, one should expect the probability for the $(d+1)$-dim hypercube to enter ground states being also close to p^2 for large d.

The above argument comparing the coupled and uncoupled dynamics is essentially investigating the correlation between the two d-dim sub-cubes, we will quantitatively study this in the next conjecture.

Conjecture 2. *(A Central Limit Theorem) The final magnetization $M_\infty(N) = M_\infty(d)$ converges in distribution to standard Gaussian under a certain scale, i.e.: there exists a function f that acts on N such that:*

$$\frac{1}{f(N)} M_\infty(N) \xrightarrow[N\to\infty]{(d)} \mathcal{N}(0,1) \tag{12}$$

The first thing one should quickly notice is that if Conjecture 2 holds to be true, Conjecture 1 would be easily yielded. Our numerical study (Fig. 3 (a) and (b)) suggests that the correct scale f should satisfy: $\sqrt{N} \ll f \ll N$. From now on, for the sake of simplicity, let's only consider d to be odd so that there's no blinkers. Given two spins $\sigma^d_{i_1}$ and $\sigma^d_{i_2}$ on a d-dim hypercube Q_d, by symmetry, the site-to-site correlation function of them should be only dependent on l, where $l = \mathbf{d}_h(i_1, i_2) \le d$, $\mathbf{d}_h$ the Hamming distance. We then define the site-to-site correlation function as $t \to \infty$ as the following:

$$C^d(l) = \lim_{t\to\infty} \langle \sigma^d_{i_1}(t), \sigma^d_{i_2}(t) \rangle, \text{ where } l = \mathbf{d}_h(i_1, i_2) \tag{13}$$

Then consider a k-renormalization of Q_d into Q_{d-k}, where each vertex j is associated to a k-dim sub-cube $Q_{k,j}$, where $k \ge \lfloor \frac{d}{2} \rfloor + 1$. For $j_1, j_2 \in Q_{d-k}$, we consider the final magnetization S_{k,j_1} and S_{k,j_2} for sub-cubes Q_{k,j_1} and Q_{k,j_2}, i.e.:

$$S_{k,j_1} = \lim_{t\to\infty} \sum_{i \in Q_{k,j_1}} \sigma^d_i(t), \tag{14}$$

therefore the correlation between the final magnetization S_{k,j_1} and S_{k,j_2} is:

$$\lim_{t\to\infty} Corr(S_{k,j_1}, S_{k,j_2}) = \lim_{t\to\infty} \frac{1}{\sqrt{Var(S_{k,j_1}) Var(S_{k,j_2})}} \sum_{i_1 \in Q_{k,j_1}} \sum_{i_2 \in Q_{k,j_2}} \langle \sigma^d_{i_1}(t), \sigma^d_{i_2}(t) \rangle, \tag{15}$$

where:

$$Var(S_{k,j_1}) = \sum_{i_1, i_2 \in Q_{k,j_1}} \langle \sigma^d_{i_1}(t), \sigma^d_{i_2}(t) \rangle \tag{16}$$

A classical argument([5]) for proving a CLT would involve showing the correlation between the final magnetization S_{k,j_1} and S_{k,j_2} vanishes as $d \to \infty$, incorporating the Fortuin–Kasteleyn–Ginibre (FKG) inequality[3]:

$$Cov(f(\sigma^d(t)), g(\sigma^d(t)) \ge 0, \text{ where } f, g \text{ are increasing functions} \tag{17}$$

There's one technical issue here: the FKG inequality above only works for configurations with positively correlated initial conditions, which is not the case for zero magnetized initial conditions. An alternate candidate which suits the case is the

symmetric i.i.d initial condition. We'll present the numerical results for the final magnetization $\tilde{M}_\infty(N)$ starting with symmetric i.i.d initial condition in the Appendix. The sample distribution of $\tilde{M}_\infty(N)$ is generally broader than $M_\infty(N)$.

An explicit formula of $C^d(l)$ would be essential for proving the vanishing of the correlation between the final magnetization S_{k,j_1} and S_{k,j_2}. We have obtained the formula for $C^3(l)$ and $C^4(l)$, but the computation became much more complicated as d grows larger due to the growing number of frozen states.

Conjecture 3. *The probability for an even d-dim hypercube to enter blinker configurations goes to 1 as $d \to \infty$, i.e.:*

$$\lim_{d \text{ even}, d\to\infty} \mathbb{P}_{\sigma(0),\omega}(|G^d| > 1) = 1 \tag{18}$$

Numerical results (Fig. 11) suggest $\mathbb{P}_{\sigma(0),\omega}(|G^d| > 1)$ grows exponentially as d increases. Intuitively, this is because there are exponentially more sites, and therefore is easier for blinkers to generate. The result in Fig. 4 also adds confidence since it shows that on high-dimension hypercubes, the distribution of local magnetization $m_\infty(d)$ has support for all allowed values rather than concentrating somewhere away from zero. If there is a limit distribution for the scaled variable $\frac{1}{d}m_\infty(d)$ that has support near zero as seems reasonable from the figure, then the probability of getting a zero, i.e. becoming a blinker, would go down as $\frac{1}{d}$ while the number of spins goes up with 2^d so it is almost sure that there will be a blinker.

Conjecture 4. *On double-copy dynamics, the final overlap of the twins is strictly between 0 and 1 as $d \to \infty$, i.e.:*

$$\lim_{d\to\infty} q_\infty(d) \in (0, 1) \tag{19}$$

In both even and odd dimensions, numerical results (Fig. 13) suggest that $q_\infty(d)$ increases monotonically, with a possible limit around $\frac{1}{2}$. Given that the number of frozen states grows exponentially fast with the dimension, the hypercube will have many possible final states whose overlap is small, hence it's implausible for the final overlap to be 1 as $d \to \infty$. At the same time, the small order of the average number of flips per site implies the double-spin dynamics can't bring the initial configuration into two final configurations that differ too much, therefore we believe the final overlap will be strictly positive as $d \to \infty$.

Appendix

Algorithm for obtaining G^d_∞ For t small, the cardinality for $G^d(t)$ is exponentially huge and useless. Therefore, one should implement the following algorithm for t large enough such that the active list $a^d(t)$ is small: The dynamics define a directed graph with vertices in $G^d(t)$, such that the directed edges correspond to any of the possible single steps of the dynamics. We can then find $G^d(t)$ by performing a Breadth First Search (BFS) starting with a root at the configuration at t, and the number of vertices at depth 1 should be $|a^d(t)|$. To determine whether $G^d(t) = G^d_\infty$, we perform a Depth First Search on $G^d(t)$ and we stop once we find a spin with energy change $\Delta E < 0$ in the configuration on a vertex, this means that $G^d(t) \neq G^d_\infty$ and the dynamics needs to be run further to find G^d_∞; otherwise if the search successfully goes through the whole tree, then $G^d(t) = G^d_\infty$.

Explicit Construction for a blinker configuration at d = 8 Set the following four 5-dim sub-cubes to be all plus, and the complement of their union to be all minus. Then we obtain a blinker configuration with a 1-blinker at the origin $\vec{0}$.

(1***|00**), (*1**|**00), (**1*|00**), (***1|**00).

Denote the union of the origin and the four 5-dim sub-cubes to be M, and N the complement of M. We will show that N is a union of 12 5-dim sub-cubes. $|M| = 88$ and $|N| = 168$, if we want to show that a certain union of 5-dim sub-cubes (which is disjoint from M) equals N, it's enough to check that its cardinality is the full 168. This can be achieved by the union of the following collection, which started as 12 5-dim sub-cubes but then 8 of them could be combined to give 4 6-dim sub-cubes:

(*0*0|1***), (*0*0|*1**), (0*0*|**1*), (0*0*|***1).

(****|1*1*), (****|1**1), (****|*11*), (****|*1*1)

We claim that these 12 5-dim sub-cubes are disjoint from M, and their union has cardinality 168, and we're done.

Counting argument for 2-blinker Suppose we are at $dim = d$, and d even. We know that one of the blinker b_1 has $\frac{d}{2} - 1$ plus nearest neighbors (NN) and $\frac{d}{2}$ minus NN's, and the other blinker b_2 has $\frac{d}{2}$ plus NN's and $\frac{d}{2} - 1$ minus NN's.

We should note that each NN's of b_1 is connected to a NN's of b_2. Therefore, we assume that each of the first $\frac{d}{2} - 1$ minus NN's of b_1 is a neighbor of a minus NN's of b_2, and each of the first $\frac{d}{2} - 1$ plus NN's of b_2 is a neighbor of a plus NN's of b_1. Finally, there is one plus NN of b_1 and one minus NN of b_2 left, and they have to be coupled together.

Now each one of the first $\frac{d}{2}-1$ minus NN's of b_1 will have $\frac{d}{2}$ like-NNN's since it is additionally connected to a minus NN of b_2, therefore requires 1 more unlike-NNN's to be stable. Each one of the $\frac{d}{2}-1$ plus NN's of b_1 will have $\frac{d}{2}-1$ like-NNN's since it is additionally connected to a plus NN of b_2, therefore requires 2 more unlike-NNN's to be stable. Finally, the minus NN of b_1 that is additionally connected to a plus NN of b_2 will have $\frac{d}{2}-1$ like-NNN's, therefore also requires 2 more unlike-NNN's to be stable. In conclusion we require $2\times((\frac{d}{2}-1)+2\times(\frac{d}{2}-1)+2)=3d-2$ number of distinct unlike-NNN's, while the total number of unlike-NNN's should be $\frac{d^2}{2}-d$. Hence we require: $\frac{d^2}{2}-d\geq 3d-2$, which gives up $d\geq 7.46$.

References

[1] Kipton Barros, P. L. Krapivsky, and S. Redner. Freezing into stripe states in two-dimensional ferromagnets and crossing probabilities in critical percolation. *Phys. Rev. E*, 80:040101, Oct 2009.

[2] Reza Gheissari, Charles M. Newman, and Daniel L. Stein. Zero-temperature dynamics in the dilute curie–weiss model. *Journal of Statistical Physics*, 172(4):1009–1028, June 2018.

[3] Theodore Edward Harris. A correlation inequality for markov processes in partially ordered state spaces. *Annals of Probability*, 5:451–454, 1977.

[4] Morávek Jaroslav Havel, Ivan. b-valuations of graphs. *Czechoslovak Mathematical Journal*, 22(2):338–351, 1972.

[5] C. M. Newman. Normal fluctuations and the fkg inequalities. *Communications In Mathematical Physics*, 74(2):119–128, June 1980.

[6] C. M. Newman and D. L. Stein. Zero-temperature dynamics of ising spin systems following a deep quench: Results and open problems. *Physica A: Statistical Mechanics and its Applications*, 279(1):159–168, May 2000.

[7] Charles Newman, Soumya Nanda, and Daniel Stein. *Dynamics of Ising spin systems at zero temperature*, pages 183–194. Amrican Mathematical Society Translations, Series II. American Mathematical Society, 2000.

[8] J. Olejarz, P. L. Krapivsky, and S. Redner. Zero-temperature relaxation of three-dimensional ising ferromagnets. *Phys. Rev. E*, 83:051104, May 2011.

[9] V. Spirin, P. L. Krapivsky, and S. Redner. Fate of zero-temperature ising ferromagnets. *Phys. Rev. E*, 63:036118, Feb 2001.

[10] V. Spirin, P. L. Krapivsky, and S. Redner. Freezing in ising ferromagnet. *Phys. Rev. E*, 65:016119, 2001.

[11] J. Ye, R. Gheissari, J. Machta, C. M. Newman, and D. L. Stein. Long-time predictability in disordered spin systems following a deep quench. *Physical Review E*, 95(4), apr 2017.

[12] J Ye, J Machta, C Newman, and Daniel Stein. Nature versus nurture: Predictability in low-temperature ising dynamics. *Physical Review. E*, 88:040101, 10 2013.